International Journal of Nanoscience
Vol. 6, No. 6 (2007) 501–513

World Scientific
www.worldscientific.com

AN INVESTIGATION INTO THE ORIGIN OF SMALL ENERGY CHANGES ($\sim 10^{-7}$ eV) OF ULTRACOLD NEUTRONS IN TRAPS

D. G. KARTASHOV
Istituto Nazionale di Fisica Nucleare, Pontecorvo, 3-56127 Pisa, Italy

E. V. LYCHAGIN*, A. Yu. MUZYCHKA*, V. V. NESVIZHEVSKY†,
G. V. NEKHAEV* and A. V. STRELKOV*
**Joint Institute for Nuclear Research, 141980, Dubna, Moscow Region, Russia*
†*Institut Laue-Langevin, 6 rue Jules Horowitz*
38000 Grenoble, France

Revised 7 September 2007

We studied the phenomenon of relatively small changes in the energy of ultracold neutrons (UCN) (when compared to thermal motion energy) when these are reflected on a surface. The changes observed involved both increases in UCN energy (their heating) and decreases (cooling) of the order of $\sim 10^{-7}$ eV. The probability values of this process on various surfaces ranged between 10^{-8} and 10^{-5} per one collision; the probability of such a small heating was many times larger than that of such a small cooling. We measured the spectra of such heated neutrons and the dependence of small heating probability on the temperature of sample out-gazing. We found that out-gazing of samples in vacuum at a temperature of 500–600 K could increase the small heating probability on stainless steel surface by a factor of ~ 100; and on copper surface by a factor of ~ 10. We observed, for the first time, extremely intensive small heating of UCN on powder of diamond nanoparticles. Neither small heating of UCN, nor nanoparticles could be found on a sapphire single crystal surface. This set of experimental data indicates that the inelastic scattering of UCN on weakly bound nanoparticles at a surface in a state of thermal motion is responsible for the process investigated.

Keywords: Ultracold neutrons; neutron lifetime; surface nanoparticles; dynamics of nanoparticles.

1. Introduction

The attractiveness of ultracold neutrons (UCN) in physics experiments is due to their capacity for long storage in closed volumes — so-called UCN traps. Since the discovery of UCN,[1] neutron loss from traps has always exceeded the theoretically expected values in UCN storage experiments. If traps are made of such low-absorbing materials as beryllium and solid oxygen, then the loss excess factor can be as high as $\sim 10^2$ and $\sim 10^3$, respectively.[2,3] This so-called "anomalous UCN loss" is one of most intriguing problems in modern neutron physics. A detailed history of this research up to 1990 can be found, for instance, in Refs. 4–6.

The traditional description of UCN interaction with matter assumes their loss from closed traps via three channels: their β-decay, their absorption by nuclei in the matter of trap walls, and their inelastic

scattering on trap walls. This third possibility assumes the most probable scattering of UCN to the energy range corresponding to the wall temperature; this value exceeds the kinetic energy of the UCN by five orders of magnitude.

Usually, UCN loss via inelastic scattering is supposed to follow from the contamination of trap walls by hydrogen. Hydrogen penetrates materials; the cross-section of inelastic neutron scattering on hydrogen is high. Hence its presence at the surface considerably increases UCN loss. Both the inelastic scattering of UCN on the surface[7,8] and the presence of hydrogen on the surface[9] have been confirmed in experiments. The energy of inelastically scattered (on copper) neutrons was measured in Ref. 7 to be equal to 5–15 meV; this energy agrees with the assumption that dominant UCN up-scattering occurs to the thermal energy range. Many experiments have studied various methods of removing hydrogen from the surface (see, for instance, Ref. 4, pp. 201–205); they have shown that the out-gazing of traps in a vacuum of $10^{-3} \times 10^{-4}$ mbar at a temperature of $\sim 400^{\circ}$C can reduce the probability of loss and is easily feasible. Out-gazing has thus become a standard procedure in the preparation of UCN storage traps.

The inelastic scattering of UCN on residual hydrogen could be reduced by cooling the trap walls. The temperature-dependence of the flux of up-scattered neutrons on a beryllium surface has been measured experimentally.[10] It has been shown that a reduction in the beryllium temperature from ~ 300 K to ~ 80 K sharply reduces the flux of up-scattered neutrons to the thermal energy range. The cross-section of the corresponding UCN loss did not exceed 15% of the anomalous loss cross-section in beryllium traps, as measured in Ref. 3. Furthermore, the investigation of UCN absorption ((n, γ) reaction) at a beryllium surface[11] reveals no additional loss commensurate with the anomalous loss. Both the experimental data in Refs. 2 and 3 therefore (in which the cross-section of UCN loss on beryllium at a temperature of 10 K was equal to ~ 1b and did not depend on temperatures in the range of 10–80 K), and the data in Refs. 10 and 11 (showing that loss probability can be explained neither by absorption nor by UCN up-scattering to the thermal energy range) contrast with the generally accepted models describing the loss of UCN as a result of their interaction with a solid surface.

Another hypothesis has long been discussed: could UCN be lost from traps as a result of the anomalously intensive inelastic scattering of UCN on a surface with an energy change smaller than the energy of the thermal motion? Several groups of experimentalists have concentrated their efforts on the search for such up-scattering. The pioneering experiment in this field has been described in Ref. 8. Such "anomalous" UCN heating was not found in the energy range of 4×10^{-7}–5×10^{-3} eV with the probability higher than 10^{-3} per collision with the surface. The search for neutron up-scattering to the energy range slightly higher than the UCN energy range[12,13] has been unsuccessful. In another experiment[14] UCN heating was not observed to the energy range of 2×10^{-6}–5×10^{-4} eV with the probability higher than 3×10^{-5} per collision with the surface.

In 1997, however, an additional mechanism for UCN loss from traps was finally discovered. The UCN energy increased by $\sim 10^{-7}$ eV with the probability of 10^{-8}–10^{-5} per collision[15]; this value exceeded theoretical expectations by many orders of magnitude. If the neutron energy after such inelastic scattering exceeds some critical value it would escape from the trap. This process is similar to the vaporization of UCN from a trap, we have therefore called such neutrons VUCN (Vaporizing UCN) and the process itself has been called the "small heating" of UCN (in contrast to the well-known heating of UCN to the thermal energy range). In Ref. 16 a reduction in UCN energy was found on the surface of hydrogen-free "Fomblin" oil.

The small heating of UCN has been studied over the last eight years both on solid surfaces (stainless steel, copper, beryllium, etc.) and on liquid surfaces (different kinds of hydrogen-free oils).[15–23] The experimental discovery of the small heating of UCN required a revision of our theories on the interaction of UCN with a surface[24] and a careful consideration of the different processes at the surface capable of providing inelastic scattering of UCN. The following mechanisms underlying small changes in UCN energy were considered: their scattering off hydrogen contamination diffusing on the surface,[25,26] their scattering at thermal fluctuations of a viscous medium,[27] their scattering at surface capillary waves,[28] and additional degrees of freedom in gravitational interaction.[29] Reference 30 provides a review of the possible reasons for the small heating of UCN. This analysis

leads to the conclusion that, in the framework of standard quantum mechanics, only the scattering of UCN at clusters with a size of ~ 100 Å can explain the complete set of experimental data obtained; the velocity of the clusters has to correspond to the observed values of energy change. In Ref. 31 the coherent interaction of UCN with the thermal motion of surface nuclei was considered in a general case; it was shown that the small heating of UCN could only be due to changes in the energy of the UCN due to their reflection from weakly bound nanoparticles at the surface in a state of permanent thermal motion. Besides, neutrons are able to "chose" nanoparticles with the size of $\sim \lambda$ (UCN wavelength) irrespective of the particular distribution of nanoparticle sizes; we can thus easily estimate the most probable value of energy change per collision as $\sim 10^{-7}$ eV at a temperature of ~ 300 K. One objective of the experiment presented here was to verify the hypothesis of a nanoparticle (cluster) origin for the small heating of UCN.

Despite the diversity of the experimental installations used for identifying and studying the small heating of UCN, they can be classified into two broad groups, depending on which of two experimental methodologies is applied.

In an installations of the first kind, as in Ref. 8 for instance, a sample is placed in a vacuum volume (the trap) surrounded by neutron detectors. UCN "irradiate" a sample and may be inelastically scattered to an energy high enough to traverse the trap walls into the neutron detector. The minimum energy of the neutrons detected in such experiments is defined by the critical energy of the trap wall material and by the neutron loss inside the trap walls. The spectrum of scattered neutrons can be measured using a multi-layer detector, in which neutrons of small energy are detected in the layers placed close to the UCN trap. Installations of this kind can be used for measuring up-scattered neutrons with energies higher than ~ 500 neV. This is the measurement methodology used in Refs. 7 and 12–14.

An installation of the second kind employs a different methodology: the storage of "heated" neutrons in a trap and their subsequent detection as normal UCN. This requires the maximum energy in the initial UCN spectrum to be significantly lower than the critical energy of the trap wall material. In addition, the storage time of the neutrons with an energy higher than the maximum energy in the initial spectrum needs to be sufficient to allow their efficient detection. The neutrons of the final spectrum are separated from the neutrons of the initial spectrum by a thin foil of specific critical energy, or by a gravitational barrier of an appropriate height. This method has been used in Refs. 15, 16, and 19–23. The initial spectrum of UCN is selected using a gravitational spectrometer. The spectrometer relies on the fact that the kinetic energy of UCN decreases by a characteristic value of $\sim 10^{-7}$ eV as it rises 1 m in the Earth's gravitational field; this defines the size of the gravitational spectrometer. If a so-called "absorber" is installed, inside the gravitational spectrometer, at a height of slightly less than 1 m, and if the UCN remain for a certain period of time in the spectrometer, nearly all neutrons with an energy of over 100 neV are removed. The "absorber" is then raised and UCN can again be stored in the spectrometer. Thereafter the spectrum of neutrons up-scattered during the storage period can be measured, by placing the "absorber" at various heights or by replacing the foil with other separation foils with different critical energies.[32] Installations of this kind can be used to detect heated neutrons with energies lower than ~ 200 neV, a figure corresponding to the maximum energy of UCN capable of storage in a spectrometer for a sufficient period of time.

2. The Experimental Installation and Measurement Method

In order to study the origins and characteristics of UCN small heating, we constructed a Big Gravitational Spectrometer (BGS) allowing the simultaneous measurement of the UCN and VUCN produced during UCN storage. The BGS provides detection in the energy range of 30–150 neV with an efficiency of $\sim 50\%$; this is an improvement on previous installations of this kind. The efficiency of VUCN detection for all energies of interest to us is physically measured rather than theoretically estimated; this provides precision and reliability for the results obtained. The spectrometer design allows for the rapid and convenient replacement of samples and the adaptation of the spectrometer for various experimental purposes. The internal spectrometer volume is separated hermetically from its external vacuum protecting volume; this allows it to be heated to 600 K or cooled to 80 K, providing measurements across a broad range of temperatures.

The essential set-up for the BGS is shown in Fig. 1. The sample (1) is placed at the bottom

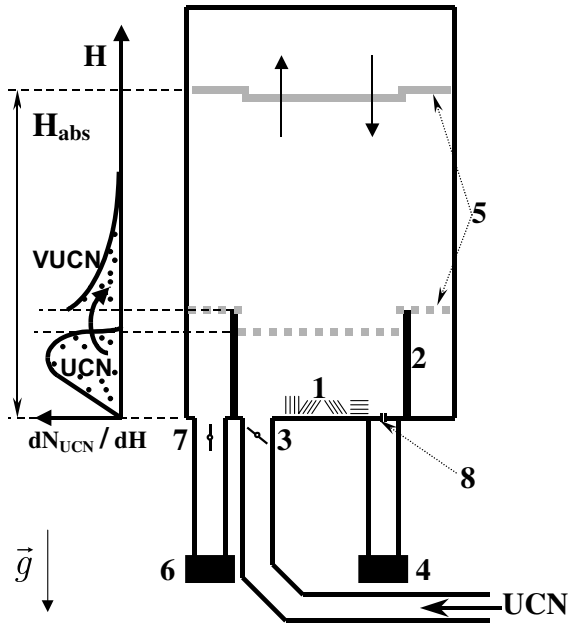

Fig. 1. Schematic diagram of experimental set up: 1 — sample, 2 — gravitational barrier, 3 — entrance valve, 4 — monitor, 5 — absorber, 6 — detector, 7 — exit valve, 8 — calibration hole. To improve legibility, the external vacuum volume is not shown.

of the spectrometer inside a 30 cm-diameter cylinder (2) forming the internal storage volume for the UCN and providing the gravitational barrier for the neutrons (the internal storage volume is in copper). The UCN enter the internal storage volume through the neutron guide inlet and are trapped inside it when the entrance valve (3) is closed. The calibration hole in the spectrometer bottom (8) allows the neutron flux density in the spectrometer to be measured using the monitor detector (4). The spectrum of stored UCN is shaped from above by placing the absorber (5) at a defined height H_{abs} (UCN energy will be defined below in cm, with reference to the maximum height of the neutrons' rise in the Earth's gravitational field). If the neutrons' energy is sufficient to raise them to a height larger than H_{abs}, they will eventually be lost in the absorber. A detector (6) is placed on the other side of the gravitational barrier (2), so that only those neutrons with energy higher than ($E_{\rm bond}$) can be detected. If the absorber is placed at its maximum height ($H_{abs} = H_{\rm max} > E_{\rm bond}$) the VUCN produced when UCN collide off the sample surface and walls of the inner storage volume can overcome the gravitational barrier. They can thus reach the detector (6) through the exit valve (7), which remains open throughout the measurement cycle. The gravitational barrier can be placed at heights of between 30 cm and 120 cm. In the experiment described we used a single gravitational barrier of a height of 50 cm.

The absorber is made of titanium alloy with negative critical energy. The UCN can penetrate this absorber to be absorbed by nuclei or up-scattered to the thermal energy. However, some UCN may be reflected back from the absorber surface into the storage volume. In order to reduce the probability of this we increased the absorber surface area and thus increased the frequency of UCN collisions with the absorber. By placing the absorber at its minimum height ($H_{abs} = H_{\rm min}$) the UCN with energy larger than the energy of the gravitational barrier are removed ($E_{\rm bond}$) if $H_{\rm min} < E_{\rm bond}$.

Figure 2 shows typical time dependencies of the detector count rate in measurements with various samples. When filling the spectrometer (between the 0 and 100 s) the entrance valve is open and the absorber is at its minimum height. Some UCN in the initial spectrum with energy exceeding the gravitational barrier can penetrate the physical gap between the absorber and the storage volume walls. They can rise above the gravitational barrier and reach the detector. This explains the high detector count rate. Soon after closing the entrance valve (100 s) these neutrons will be lost in the absorber; this explains the sharp decrease in the detector count. Some tens of seconds are sufficient

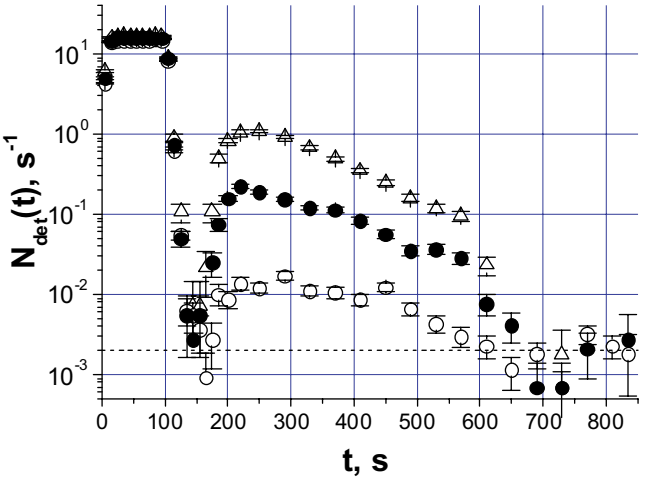

Fig. 2. Time evolution curve of the detector count rate. White circles represent the measurement of VUCN production at the surface of an empty copper spectrometer. Black circles represent the measurement with a stainless steel sample. Triangles represent the measurement with diamond nanoparticles. The dashed line represents the background level.

for removing UCN with energy higher than the gravitational barrier, allowing the detector count rate to fall to the background level. If at the 170 s the absorber is raised to its maximum height then the detector count rate will start rising to become proportional to the UCN flux in the spectrometer. This dependence is explained by the permanent production of VUCN with energy higher than the gravitational barrier. At the 590 s the absorber is lowered to its minimum height and the detector count rate falls to the background value.

Statistics are collected by repeating these measurement cycles. The fraction of the measurement cycle presented below between the closure of the entrance valve and the lifting of the absorber is called "cleaning"; the fraction of the measurement cycle between the lifting of the absorber and its return to minimum height is called the "main part" of the measurement cycle. The design of the installation does not allow detection of any neutrons other than VUCN during the main part of the measurement cycle.

Figure 3 illustrates some of the characteristics of the BGS: the spectra of UCN with energy smaller than the gravitational barrier, and UCN storage times at room temperature.

Let us now define the quantities needed for further description. The probability of small heating P_{VUCN} is the probability of a change in UCN energy from the interval below the gravitational barrier ($E_{\text{bond}} = 50\,\text{cm}$) to the interval $E_{\text{bond}} < E_{VUCN} < 150\,\text{cm}$ at one collision of UCN with the sample surface — the upper limit for this interval is defined by the critical energy of the material of the spectrometer walls as well as by the maximum height to which one can raise the absorber. In this case,

$$P_{VUCN} = \frac{N_{VUCN}}{N_{coll}} = \frac{N_{det}}{N_{coll}\varepsilon}\,. \qquad (1)$$

Here N_{VUCN} is the number of UCN produced per measurement cycle. N_{coll} is the total number of collisions of UCN with the sample surface per measurement cycle. N_{det} is the number of detector counts per main part of the measurement cycle minus the detector background. ε is the efficiency of VUCN detection.

The samples to be investigated are placed at the bottom of the spectrometer. Sample height does not exceed a few cm. The UCN flux measured in the monitor detector through the small hole in the spectrometer bottom is therefore almost equal to the UCN flux at the sample surface. This explains why Eq. (1) can be written as follows:

$$P_{VUCN} = \frac{N_{det}S_{mon}}{N_{mon}S\varepsilon}\,. \qquad (2)$$

Here N_{mon} is the number of counts in the monitor detector during the main part of the cycle. S is the area of sample surface. S_{mon} is the area of the small hole in the spectrometer bottom, through which the

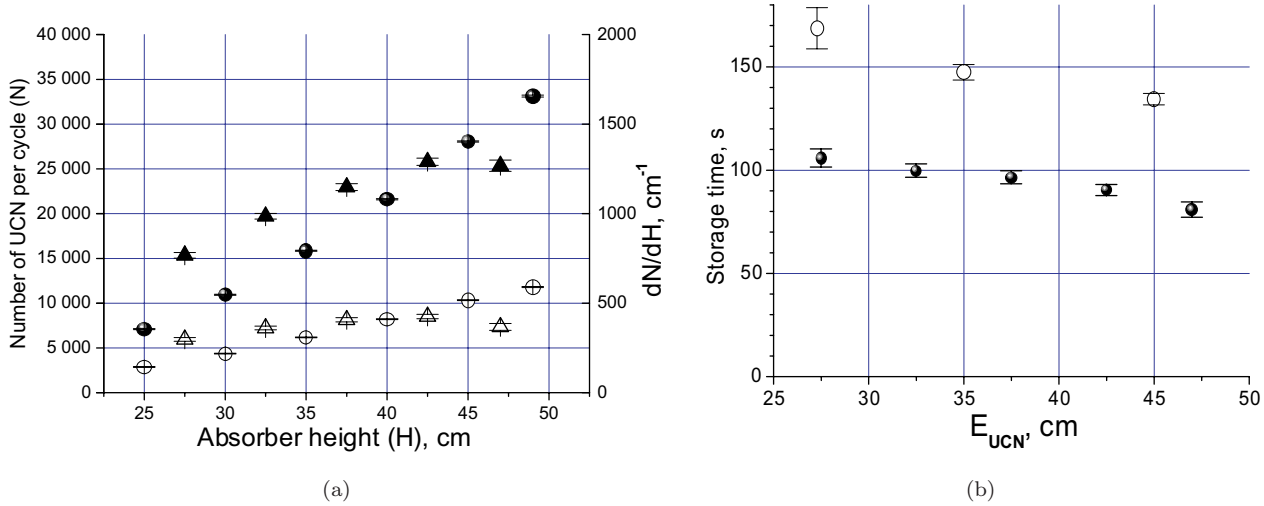

(a) (b)

Fig. 3. Plot of characteristics of the BGS. (a) Integral and differential spectra of UCN in the spectrometer with stainless steel samples of 0.7 m^2 area. All circles (left axis) show the number of UCN in the spectrometer as a function of absorber height (integral spectra). All triangles (right axis) indicate the result of the numerical differentiation of the integral spectra. Black corresponds to the UCN spectrum at the 42 s after closure of the entrance valve. White corresponds to the UCN spectrum at the 142 s after closure of the entrance valve. (b) UCN storage time in the spectrometer as a function of their energy. White corresponds to data with the spectrometer empty. Black corresponds to spectrometer with a stainless steel sample.

UCN can reach the monitor. If P_{VUCN} is defined as above and the monitor detector is equivalent to the main detector, the efficiency ε will be equal to the fraction of detected VUCN over the number of VUCN produced (including the UCN which were lost in the spectrometer by the end of the main part of the measurement cycle):

$$\varepsilon = \frac{\tau_{det}^{-1}}{\tau_{VUCN}^{-1}} = \frac{\tau_{det}^{-1}}{\tau_{\rm stor}^{-1} + \tau_{det}^{-1}}\,. \qquad (3)$$

Here τ_{det} is the time required for the UCN to empty from the spectrometer to the detector. τ_{VUCN} is the period for which the VUCN are stored in the spectrometer with the exit valve open. $\tau_{\rm stor}$ is the period for which the VUCN are stored in the spectrometer with the exit valve closed. The values τ_{det} and $\tau_{\rm stor}$ depend on VUCN energy; therefore the efficiency ε also depends on energy. If the dependencies $\tau_{det}(E)$ and $\tau_{\rm stor}(E)$ are measured, then the efficiency $\varepsilon(E)$ can be calculated.

Figure 4 shows the results after measuring of the energy dependence of VUCN detection efficiency in the empty spectrometer and in the spectrometer holding a stainless steel sample at room temperature.

As detection efficiency depends on VUCN energy, knowledge of the spectrum is indispensable for determining P_{VUCN}. Figure 5 indicates the number of detected VUCN N_{det} per measurement cycle, as a function of maximum absorber height

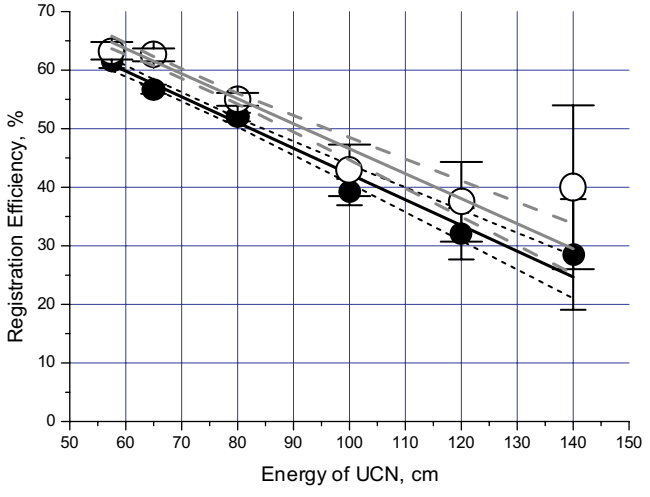

Fig. 4. The plot of dependence of detection efficiency on VUCN energy. The white circles correspond to VUCN detection efficiency $\varepsilon(E)$ in the empty spectrometer. The black circles represent the efficiency $\varepsilon(E)$ in the spectrometer with the stainless steel sample. The solid and dashed lines indicate their linear fits and 70% confidence intervals, respectively.

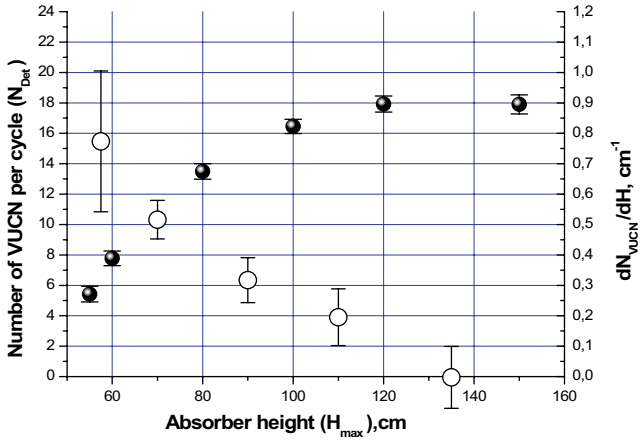

Fig. 5. VUCN spectra in the spectrometer with a stainless steel sample. The black circles (left axis) correspond to the "integral" VUCN spectrum. The white circles correspond to the "differential" VUCN spectrum.

$H_{\max}$ (black circles); the minimum absorber height $H_{\min}$ was equal to 44 cm. The observed dependence could be described as follows:

$$N_{det}(H_{\max}) = \int_{E_{\rm bound}}^{H_{\max}} \frac{dN_{VUCN}}{dE}\varepsilon(E)dE\,. \qquad (4)$$

The differential VUCN spectrum dN_{VUCN}/dE can therefore be calculated using numerical differentiation of the dependence $N_{det}(H_{\max})$. The result must be divided by the measured dependence $\varepsilon(E)$. The final result is presented in Fig. 5 (white circles).

Equation (4) is accurate if neutrons with energy higher than the absorber height $H_{\max}$ are not detected. However, a fraction of the neutrons with energy higher than $H_{\max}$ are counted by the detector if they are not lost in the absorber. Usually these are neutrons with energy slightly higher than $H_{\max}$. Strictly speaking, all these experimental values need to be corrected before numerical differentiation of $N_{det}(H_{\max})$. The differential spectrum would therefore be slightly different from the spectrum calculated using experimental data without correction. The precise calculation of the corrections is complicated. However, the corrections can be estimated by comparing the cleaning time $\tau_{\rm clean}(E)$ and the emptying time $\tau_{det}(E)$ for the VUCN with energy higher than $H_{\max}$. Thus, for instance, if the absorber is installed at a height of 60 cm, the emptying time for neutrons with energy higher than 65 cm will be equal to $\tau_{\rm clean} \sim 5$ s and the emptying time will be equal to $\tau_{det} \sim 60$ s; for the absorber height of 130 cm and for neutrons with energy higher than 140 cm these times will be equal to $\tau_{\rm clean} \sim 10$ s

and $\tau_{det} \sim 90$ s. Thus, such neutrons are not lost in the absorber but are detected with a probability of $\sim 10\%$. This probability depends strongly on the difference between the VUCN energy and $H_{\max}$. We therefore consider that corrections for data in the dependence $N_{det}(H_{\max})$ (in Fig. 5) do not exceed 10% and we have not taken them into account when calculating the differential spectra.

VUCN spectra measured with other samples and with other UCN energies (other values of $H_{\min}$), do not differ significantly from the spectra presented. VUCN detection efficiency for various other samples also corresponds closely (see. Fig. 4). The reason for this coincidence is that the storage time τ_{stor} (see. Eq. (3)) is largely defined by neutron losses in the spectrometer walls and not in the samples; τ_{det} is the same in all cases. Therefore, if the spectrometer were to receive no special treatment (cooling, for instance, or long out-gazing) we could assume that the VUCN spectrum is the same as that presented in Fig. 5, and the dependence $\varepsilon(E)$ is the same as that presented in Fig. 4. The average efficiency of VUCN detection was equal to $\varepsilon \sim 50\%$. All the probabilities presented below for small heating P_{VUCN} were estimated for efficiency value $\varepsilon = 50\%$.

Before each measurement all parameters of the installation need to be selected in order to avoid false effects.

The experimental data can be presented as the time evolution of the ratio of neutron count rate (flux of detected VUCN) to monitor count rate. Figure 6 shows this ratio for the samples presented in Fig. 2. One should note that the small value for the effect being studied suggests that the UCN spectra at the samples need to be treated with caution. In particular, any mechanical motion inside the storage volume (e.g., the closing or opening of valves) once UCN spectrum shaping is complete (after spectrum cleaning) would produce false heating of UCN. We therefore avoided any mechanical movement other than lifting the absorber. The raising of the absorber does not itself affect the UCN spectrum, as any neutron with sufficient energy to rise to the absorber will have been absorbed by the time the absorber is raised (during spectrum cleaning). Besides, any such false effect would render the neutron count rate much more time dependent (compared to measurements with the monitor detector), given the short storage time of high-energy neutrons. The ratio of the detector/monitor count rates would show no tendency

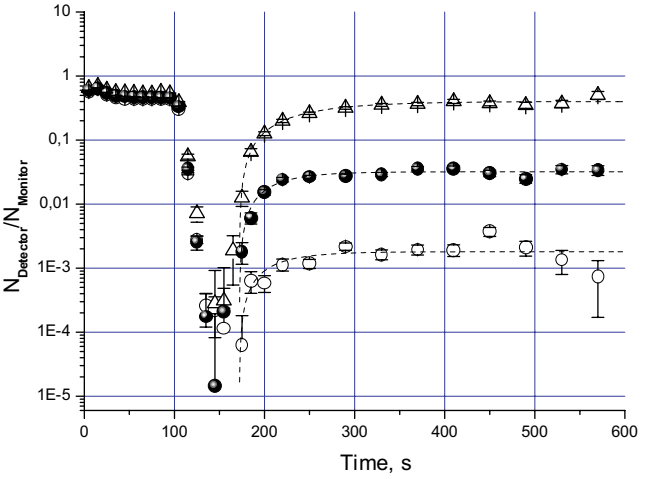

Fig. 6. Plot of neutron count rate divided by monitor count rate versus time. The white circles correspond to the measurement with an empty copper spectrometer. The black circles correspond to the measurement with a stainless steel sample inside the spectrometer. The triangles represent the measurement with a powder of diamond nanoparticles.

to be constant at high time values (see. Fig. 6), but would decrease with time.

There are two other false effects to be avoided. The first could result from UCN with energy lower than the gravitational barrier $E_{UCN} < E_{\text{bond}}$ crossing from the internal part of the spectrometer through flaws in the gravitational barrier seal. This can be checked by measuring as for a standard cycle but with the absorber fixed at its minimum height permanently (a few centimetres below the upper edge of the gravitational barrier). If the neutron count rate does not exceed the background level during the main part of the cycle there is no false effect. These checks were carried out a few times during the experiment; no false effect was found.

The second possible false effect concerns residual UCN with energy higher than the gravitational barrier and not completely removed when the absorber is raised. Figure 7 shows the number of detected neutrons per measurement cycle (during the main part of the cycle) as a function of cleaning time. If the corresponding false effect is absent, the neutron count rate will be proportional to the monitor count rate. For demonstration purpose, the number of neutrons counted by the monitor detector (during the main part of the cycle) is normalized to the number of neutrons counted by the main detector. Evidently, if the cleaning time is shorter than 50 s, the monitor counts will not be proportional to the main detector counts; however,

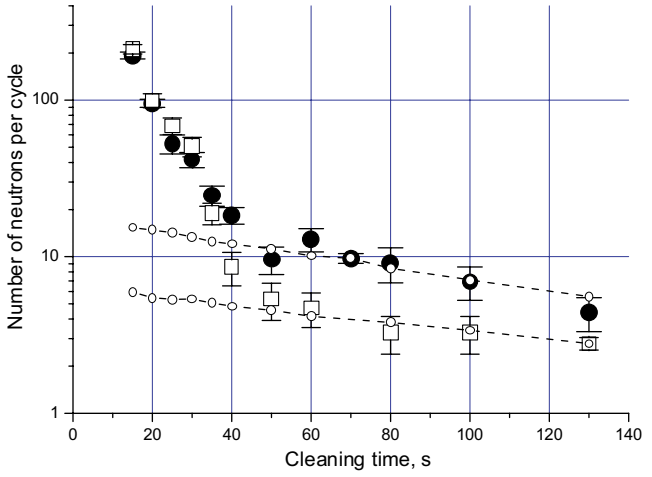

Fig. 7. Plot of the number of neutrons detected per measurement cycle as a function of spectrum cleaning time. $H_{\min} = 40$ cm. The white squares correspond to measurements with an empty spectrometer. The black circles indicate measurements with a stainless steel sample. The dashed lines and white circles show the (normalized) number of neutrons counted in the monitor detector.

if cleaning time is higher than 50 s the false effect in question will be absent.

Another way of checking for the above-mentioned false effect is to measure the small heating probability as a function of minimum absorber height $H_{\min}$. Figure 8 shows this measurement with a stainless steel sample. If this height is smaller than 45 cm, the measured dependence will be weak, and nearly linear. In the vicinity of the gravitational barrier (50 cm) a sharp increase of probability can be observed due to the above-mentioned false effect.

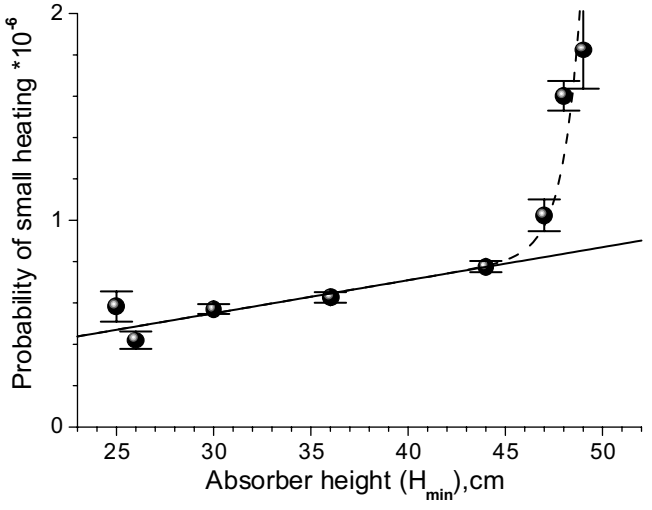

Fig. 8. Plot of probability of small heating of UCN at a stainless steel sample as a function of minimum absorber height. The time of cleaning is 70 s.

The exponentially increasing dashed curve in Fig. 8 describes experimental data at an absorber height of over 50 cm; residual above-barrier neutrons are clearly present. Thus, if the minimum absorber height is lower than 45 cm the false effect will be absent.

In other words, if the cleaning time is longer than 50 s, and the minimum absorber height is lower than 45 cm, there are no residual above-barrier UCN (above the gravitational barrier). We used a cleaning time of 70 s and a minimum absorber height $H_{\min}$ of 44 cm.

3. Results

The aim of this experiment was to reveal the origins of the phenomenon of small heating of UCN when they interact with solid surfaces. It was also to verify whether the probability of small heating depends on the procedures and parameters of sample surface treatment. Therefore a significant proportion of the measurements involved stainless steel samples, providing high probability of small heating (see Refs. 15, 19, and 20).

Figure 9 shows the results of the measurement of the probability of small heating of UCN on a stainless steel surface at various sample pre-heating temperatures. The samples consisted of spirals of foils 0.1 mm thick with a surface area of $\sim 0.3\,\mathrm{m}^2$ ("GoodFellow", alloy AISI 304, weight composition: Fe, C–0.049%, Cr–18.2%, Ni–8.66%, Si–0.58%, Mn–1.04%, P–0.021%, S–0.007%). The out-gazing (pre-heating) of the samples was carried out in a quartz furnace at constant temperature for five hours under a residual vacuum pressure of

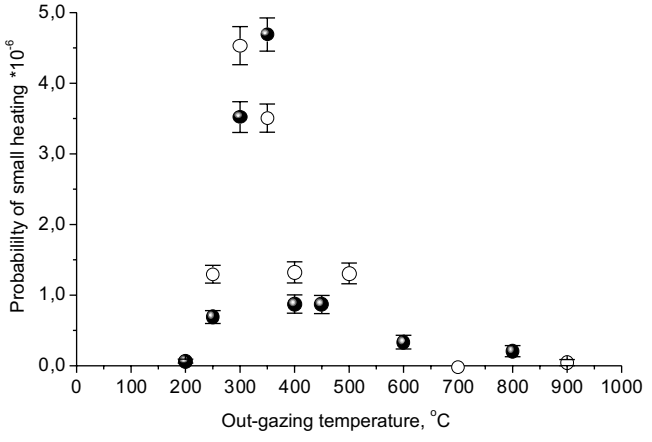

Fig. 9. Plot of probability of small heating of UCN at stainless steel samples (alloy AISI 304) as a function of the temperature of their out-gazing.

$\sim 10^{-5}$ mbar. When the samples had cooled they were transported to the spectrometer in a volume filled with inert gas. The probability P_{VUCN} was measured at room temperature. The measurement was repeated with a second but identical sample. The black and white circles in Fig. 9 correspond to the measurements with the first and second sample, respectively.

The results suggest several important conclusions. First, the probability of small heating at one sample can vary by more than two orders of magnitude as a function of the temperature of its out-gazing. Second, the dependence in Fig. 9 was reproduced twice; it is not random. Third, the maximum values of P_{VUCN} observed are of the same order as those of the "anomalous" UCN losses ($\sim 10^{-5}$), showing that they cannot be neglected in analyzing experiments on UCN storage.

An investigation of the sample surface using an atomic-force microscope (AFM) showed that the out-gazing of the stainless steel samples under study is accompanied by the formation of a small-granular structure with a characteristic grain size of ~ 10 nm. These nanostructures almost cover the surface (see Fig. 10). These facts confirm the hypothesis that the small heating of UCN is due to nanostructures (nanoparticles) on the surface. Reference 31 describes the mechanism of UCN interaction with nanoparticles; in this case the nanoparticles must be weakly bound to the surface. The probability of observed small heating of UCN ($P_{VUCN} < 10^{-5}$) corresponds to a fraction of 1 weakly bound grain per hundred thousand. Unfortunately, AFM measurement cannot distinguish weakly bound from strongly bound nanoparticles.

In order to verify the dependence of small heating probability on the procedures and parameters of treatment for other materials, we measured the production of VUCN in an empty copper spectrometer

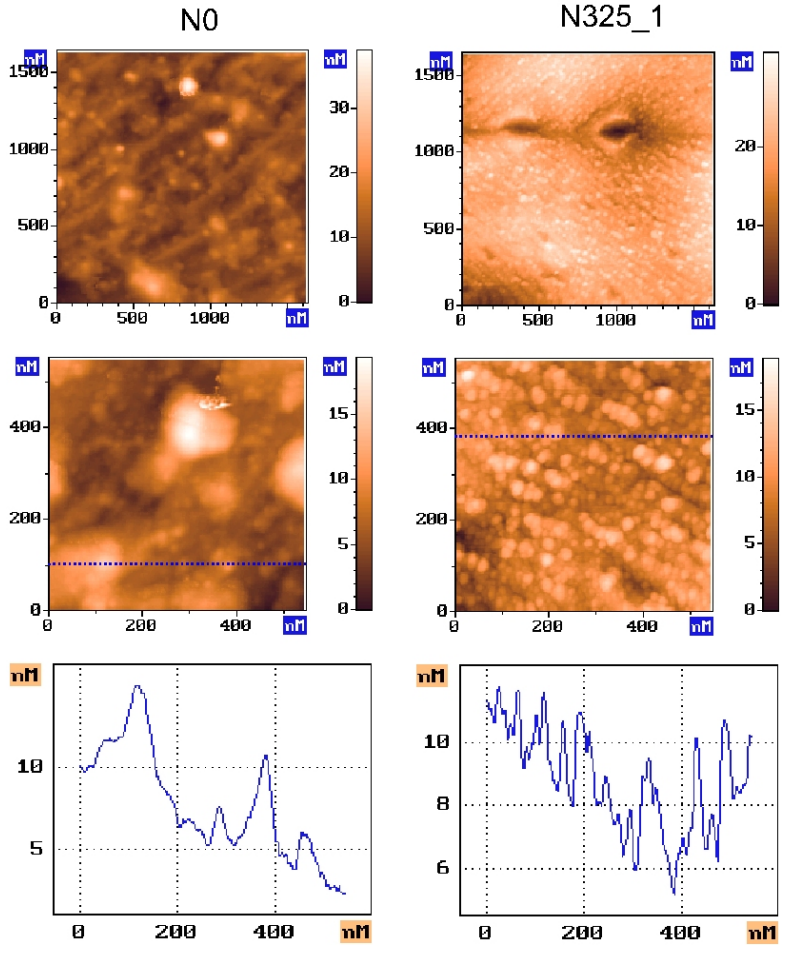

Fig. 10. Images of a stainless steel sample surface (alloy AISI 304) measured using an atomic-force microscope. The images on the left show the surface before out-gazing; those on the right show the surface after out-gazing for 5 h at a temperature of 325°C. The charts show the profiles of the surface at the dotted lines in the photos above.

Table 1. Examples of the dependence of the probability P_{VUCN} on the sample treatment procedure.

Spectrometer surface (Cu)	P_{VUCN} $\times 10^{-7}$	Stainless steel 12X18H10T	P_{VUCN} $\times 10^{-7}$
Out-gazing at 250°C	1.4 ± 0.2	Out-gazing at 400°C	1.7 ± 0.2
Second out-gazing at 250°C	1.6 ± 0.09	Out-gazing at 650°C	1.0 ± 0.2
Out-gazing at 400°C	12.9 ± 0.7	Chemical treatment in HF and out-gazing at 400°C	6.3 ± 0.4

with samples made of another kind of stainless steel.

Some of the results for the measurement of P_{VUCN}, for copper and stainless steel samples of 12X18H10T composition (Fe, C–0.12%, Cr–18%, Ni–10%, Ti–1%) are shown in Table 1. The first and third columns of the table indicate the surface treatment procedure used prior to taking neutron measurements.

The measurements with a stainless steel sample in Table 1 were carried out before the discovery of the strong dependence of small heating probability on the out-gazing temperature; the "steps" in the temperature dependence measurement are therefore too large.

The probability of small heating P_{VUCN} after out-gazing at ~ 400°C rose by a factor of ~ 10 on the copper surface (internal spectrometer surface). As is clear from Table 1, chemical treatment in aggressive substances could also significantly increase the probability P_{VUCN}.

The probabilities measured here of small changes in the energy of UCN differ from those obtained in Ref. 21 for the following reasons:

(i) The range of final VUCN energies in Ref. 21 (80–160 cm) was narrower than that in our BGS (50–160 cm). This is because a foil was used in Ref. 21 to separate the initial and final neutron energies. This is important, since about a half of the VUCN in our experiment show energy in the range (50–80 cm).

(ii) In Ref. 21 the differential spectrum of VUCN was not measured. Therefore the probability of VUCN detection was related to an energy range, and not at all to the actual VUCN spectrum. This could change the estimation of the small heating probability by a large factor.

(iii) The equation for the efficiency of VUCN detection with a given energy in Ref. 21 does not take into account any loss of neutrons with this specific energy during the counting period; this led to an overestimation of the efficiency value.

It should be noted that the results in Ref. 23 were obtained using the same installation and method as those in Ref. 21. Remarks 2 and 3 above are therefore valid for this reference as well.

In order to verify the hypothesis that the small heating of UCN is due to hydrogen contamination at the surface,[26] in addition to measuring the probabilities P_{VUCN} in Fig. 9, we also measured the probabilities P_{VUCN} and loss factors μ for similar samples of a larger size. The results are shown in Table 2. Samples No. 1 and No. 2 are identical. The last column of the table shows the results of the measurement of loss factor η.

One should note first that the dependence of P_{VUCN} on the loss factor defies the expectation in Ref. 26, and, secondly, that the experimental value for the loss factor after out-gazing at 450°C is close to its theoretical expectation, taking absorption $\eta_{\text{Teop}} \sim 1 \times 10^{-4}$ into account. The amount of hydrogen at the surface is therefore too small to provide the probability of $\sim 10^{-6}$ per collision with a surface that is required for the small heating of UCN.

The hypothesis that small heating of UCN is due to the interaction of UCN with weakly bound nanoparticles at a surface can also be tested by measuring the probability of small heating of UCN on a surface that is free of nanoparticles. The best candidates for such materials are single crystals, as

Table 2. Examples of simultaneous measurement of the probability P_{VUCN} and the loss factor μ.

Sample $S = 0.7\,\text{m}^2$	Out-gazing temperature, °C	$P_{VUCN} \times 10^{-7}$	$\mu(\langle \text{E} \rangle) \times 10^{-4}$	$\eta \times 10^{-4}$
No. 1	200	-0.2 ± 0.15	3.10 ± 0.04	5.40 ± 0.07
No. 1	450	12.7 ± 0.22	0.81 ± 0.05	1.41 ± 0.08
No. 2	200	0.2 ± 0.3	1.92 ± 0.04	3.35 ± 0.07
No. 2	450	4.9 ± 0.22	0.70 ± 0.03	1.22 ± 0.05

their surfaces are free from both hydrogen contamination and nanoparticles.

The single crystal sapphire (Al_2O_3), for instance, satisfies these conditions. An examination of its surface using an atomic-force microscope revealed no nanoparticles.

Table 3 shows the results of the measurement of the small heating probability and UCN loss probability at the surface of a sapphire sample. The sample consists of a set of single crystal plates 6 cm wide, 2 mm thick, with total surface of 1 m^2. The measurement was carried out at room temperature. The small heating probability did not exceed $\sim 10^{-8}$ per collision with a surface. The measured loss probability was larger than the theoretical absorption probability by a factor of ~ 20 (for absorption $\eta_{\text{Teop}} \sim 5 \times 10^{-6}$). This difference is apparently explained by the low temperature of the sample outgazing inside the spectrometer; the design of the BGS allows for the maximum out-gazing temperatures given in Table 3. Besides, in order to calculate the loss of neutrons in a sample, the UCN loss in the empty spectrometer has also to be taken into account; if the losses in a sample are low the accuracy of the loss probability measurement will also be low. We are therefore planning to carry out a dedicated experiment on the measurement of UCN storage time in a single crystal sapphire trap.

Yet another method to check the hypothesis of a nanoparticle origin for small UCN heating is to measure the small heating of UCN in a powder of nanoparticles. The hypothesis would be valid if the probability of small heating on a surface coated with a powder of nanoparticles is found to be much higher than without nanoparticles.

A powder (with the total volume of $\sim 3\,cm^3$) of diamond nanocrystals with an average size of ~ 50Å (produced by Ultradiamond Technologies Inc.[33]) was therefore placed on the copper bottom of the spectrometer. The powder was uniformly distributed over an area of $\sim 200\,cm^2$. The triangles in Fig. 2 correspond to the neutron count rate as a function of time. The number of VUCN is higher than that in the empty spectrometer by two orders of magnitude; although the total area of the spectrometer accessible to UCN is larger by a factor of ~ 20 than the area coated with the nanoparticle powder. If we neglect any penetration of the UCN into the powder, we can estimate the small heating probability to be equal to $P_{VUCN} \sim 10^{-3}$ and UCN loss probability at $\mu \sim 10^{-2}$.

We do not know the fraction of weakly bound nanoparticles, which would effectively increase UCN energy. Nor do we know whether UCN interact with single nanoparticles or with their ensembles. We cannot therefore yet provide a quantitative description of the process of neutrons interaction with a powder. However, the scattering of the UCN on powder of this type is a good demonstration of the small heating phenomenon itself.

Figure 11 shows the number of VUCN per main part of the measurement cycle as a function of maximum absorber height, normalized to the number of counts in the monitor detector, for a measurement involving diamond nanoparticles at the temperatures of 300 K and 108 K. As the number of counts

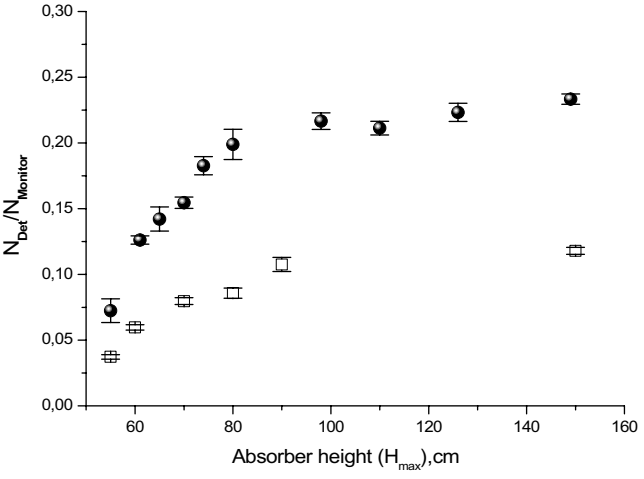

Fig. 11. Plot of measurement results with a powder of diamond nanoparticles: the number of VUCN as a function of maximum absorber height, normalized to the number of monitor counts (per main part of the measurement cycle). The black circles correspond to the measurement at room temperature. The white squares indicate measurement at 108 K.

Table 3. Results of simultaneous measurement of the probability P_{VUCN} and the loss factor μ for the sapphire surface.

Sample	Out-gazing temperature	$P_{VUCN} \times 10^{-7}$	$\mu(\langle E \rangle) \times 10^{-4}$	$\eta \times 10^{-4}$
Sapphire, $S = 1\,m^2$	200°C	0.0 ± 0.12	0.66 ± 0.01	0.97 ± 0.015

in the monitor detector (per main part of measurement cycle) does not depend on $H_{\max}$, we can compare the results presented to the dependence $N_{det}(H_{\max})$ for stainless steel (in Fig. 5). The shapes of these dependencies are very similar to each other. However, in order to calculate the differential spectrum corresponding to the data in Fig. 11 and compare it to the VUCN spectra for stainless steel, we have to measure the efficiency of VUCN detection for the nanopowder experiment.

The number of VUCN per main part of the measurement cycle, normalized to the number of counts in the monitor detector, is proportional to the small heating probability (see Eq. (2)). As follows from Fig. 11, this ratio decreased by a factor of approximately two when the temperature dropped from room temperature to the temperature of liquid nitrogen; this is approximately equal to the drop in the small heating probability measured in Refs. 19 and 20 for beryllium. However, a precise comparison is only possible after measuring the VUCN detection efficiency.

Let us return to consider the VUCN spectrum in Fig. 5 (white circles). In spite of significant statistical uncertainties, the number of VUCN is evidently lower at higher energies. The average VUCN energy in Fig. 5 is equal to 80 cm. The spectrum measurement contains systematic error. We estimate that the correction required for the average energy is less than a few centimeters. The average initial UCN energy is ~ 30 cm; the average energy change is thus equal to ~ 50 cm. This does not mean that energy changes larger than 1 m are absent. The VUCN spectrum may extend to higher energies, as far as ($\sim$ 10–15 M) even. It is possible also that the number of VUCN with energy > 1 m could be larger than the number of VUCN with energy < 1 m. This however cannot be verified using a spectrometer like the BGS, as the BGS is essentially insensitive to neutrons with energy > 1.6 m.

An important conclusion was drawn from the analysis of the differential VUCN spectrum: small heating takes place for one collision but it does not accumulate in a mini-step process. In fact, if the energy change occurs in two steps, for example, (bearing in mind the probability of $P_{VUCN} \sim 10^{-6}$–10^{-7} of small heating to the final energy) the probability of one-step heating has to be equal to $\sim 10^{-3}$; the energy dependence has to be much higher than the one measured. Besides, the value of this probability would exceed the total UCN loss probability, which is not possible.

4. Conclusion

Let us review main results:

(1) We have observed small heating of UCN; this is a one-step process with average increase in energy of ~ 50 neV.
(2) The probability of small heating of UCN on a stainless steel surface and on copper can depend heavily on sample treatment (the temperature of sample out-gazing, chemical treatment). The maximum probability in our case was equal to $(4.5 \pm 0.3) \times 10^{-6}$ per collision.
(3) At temperatures accompanied by a sharp increase in the probability of small heating of UCN, nanostructures are formed on the sample; their characteristic size is ~ 10 nm.
(4) The phenomenon observed cannot be explained by hydrogen contamination of surface (the probability P_{VUCN} and the loss coefficient μ are not correlated).
(5) Measurements with a monocrystal sapphire showed that no small heating occurs if there are no nanoparticles present in the surface.
(6) If a powder of nanoparticles is placed on the surface, the probability of small heating will increase by a few orders of magnitude; spectral and temperature dependencies of the small heating are analogous to those for metal samples.

These results confirm the hypothesis that small heating of UCN results from the interaction of UCN with weakly bound nanoparticles on a surface in a state of thermal motion.[31] The mechanisms of the interaction of the nanoparticles with the surface and with each other are not clear. We are going to produce nanoparticles at the sample surfaces with known density and bonding so that the nanoparticles do not interact with each other.

On the basis of these results we can conclude as follows. In experiments with UCN (in the neutron lifetime measurements, for instance), in which small heating could produce significant systematic errors, care has to be taken with regards to the choice of trap wall materials and trap preparation procedures. There is a need to verify whether the "anomalous" loss of UCN in Ref. 3 can be explained by their small heating.

The discovery of the inelastic scattering of UCN on nanoparticles opens up new possibilities for the use of UCN in applied research. UCN could be

employed, for example, to study the dynamics of nanoparticles and nanostructures, a use hitherto considered impossible. The inelastic scattering of UCN on nanoparticles could also be used for the thermalization of neutrons to ultra-low temperatures — a new means of achieving high UCN density.[31]

Acknowledgments

We are sincerely grateful to H. Börner, T. Butterworth, P. Geltenbort, P. Gurzhyants, V. Kurlov, I. Snigireva, V. Shashkin, N. Vostokov and A. Barabanov for their help and useful discussions.

This work is supported by the RFFI (grants nos. 00-02-17772 and 03-02-16784), and INTAS (grant no. 99-00508).

References

1. V. I. Luschikov, Y. N. Pokotilovsky, A. V. Strelkov and F. L. Shapiro, *JETP Lett.* **9**, 23 (1969).
2. P. Ageron, *Z. Phys. B* **59**, 261 (1985).
3. V. P. Alfimenkov *et al.*, *JETP Lett.* **55**, 84 (1992).
4. V. K. Ignatovich, *The Physics of Ultracold Neutrons* (Clarendon Press, Oxford, 1990).
5. R. Golub, D. J. Richardson and S. K. Lamoreaux, *Ultracold Neutrons* (Adam Higler, Bristol, 1991).
6. A. V. Strelkov, *Lectures of IV International School on Neutron Physics*, Alushta, 8-18 October 1990, JINR D3,14-91-154, Dubna (1991), p. 325.
7. A. D. Stoika, A. V. Strelkov and M. Hetzelt, *Z. Physik B* **29**, 349 (1978).
8. A. V. Strelkov and M. Hetzelt, *JETP* **47**, 11 (1978).
9. W. A. Lanford and R. Golub, *Phys. Rev. Lett.* **39**, 1509 (1977).
10. V. K. Ignatovich *et al.*, Experiments on UCN storage in bottles in the channel mode, *Communication of JINR* (1982) P3-82-811, 11.
11. A. Fomin *et al.*, *NIM A* **440**, 690 (2000).
12. A. V. Strelkov *et al.*, *Proc ISINN-4*, Dubna (1996), p. 299.
13. V. E. Varlamov *et al.*, *JETP* **87**, 417 (1998).
14. A. Yu. Muzychka, Yu. N. Pokotilovski and P. Geltenbort, *JETP* **88**, 79 (1999).
15. V. V. Nesvizhevsky, A. V. Strelkov, P. Geltenbort and P. S. Iaydjiev, *ILL Annual Report* (1997), p. 62; *Eur. Phys. J. Appl. Phys.* **6**, 151 (1999); *Phys. Atom. Nucl.* **62**, 776 (1999).
16. L. Bondarenko, P. Geltenbort, E. Korobkina, V. Morozov, Yu. Panin and A. Steyerl, *JETP Lett.* **68**, 691 (1998).
17. S. S. Arzumanov, V. I. Morozov, Yu. N. Panin, L. N. Bondorenko, P. Geltenbort and V. V. Nesvizhevsky, *Proc. ISINN-10* (2002), p. 356.
18. L. N. Bondarenko, E. I. Korobkina, V. I. Morozov, Yu. N. Panin and P. Geltenbort, *Phys. Atom. Nucl.* **65**, 11 (2002).
19. E. V. Lychagin, A. Yu. Muzychka, V. V. Nesvizhevsky, G. V. Nekhaev, R. R. Taldaev and A. V. Strelkov, *Phys. Atom. Nucl.* **63**, 609 (2000).
20. E. V. Lychagin *et al.*, *JINR* Preprint P3-2001-49 (2001); *Surface: Rentgen, Synchrotron and Neutron Investigations* **7**, 81 (2002) (in Russian).
21. A. P. Serebrov, J. Butterworth, M. Daum, A. K. Fomin, P. Geltenbort, K. Kirch, I. A. Krasnoschekova, M. S. Lasakov, Y. P. Rudnev, V. E. Varlamov and A. V. Vassiljev, *Phys. Lett. A* **309**, 218 (2003).
22. E. V. Lychagin, D. G. Kartashov, A. Yu. Muzychka, V. V. Nesvizhevsky, G. V. Nekhaev and A. V. Strelkov, *Phys. Atom. Nucl.* **65**, 1995 (2002).
23. A. Steyerl, B. G. Erozolimsky, A. P. Serebrov, P. Geltenbort, N. Achiwa, Yu. N. Pokotilovski, O. Kwon, M. S. Lasakov, I. A. Krasnoshchokova and A. V. Vasilyev, *Eur. Phys. J. B* **28**, 299 (2002).
24. A. L. Barabanov and S. T. Belyaev, *Eur. Phys. J. B* **15**, 59 (2000).
25. Yu. N. Pokotilovskii, *Eur. Phys. J. B* **8**, 1 (1999).
26. Yu. N. Pokotilovskii, *JETP Lett.* **69**, 91 (1999).
27. Yu. N. Pokotilovski, *Phys. Lett. A* **255**, 173 (1999).
28. S. K. Lamoreaux and R. Golub, *Phys. Rev. C* **66**, 044309 (2002).
29. A. Stepaniants, D. Sarkisov, A. Meyerovich and A. Steyerl, *J. Low Temp. Phys.* **113**, 1159 (1998).
30. M. Utsuro and V. K. Ignatovich, *NIM A* **440**, 709 (2000).
31. V. V. Nesvizhevsky, *Phys. Atom. Nucl.* **65**, 400 (2002).
32. Yu. N. Pokotilovskii and G. F. Gareeva, *Instrum. Exp. Techn.* **46**, 13 (2003).
33. http://www.ultradiamondtech.com/products.html.